Journal of Computational and Applied Mathematics 227 (2009) 102–114

Contents lists available at ScienceDirect

Journal of Computational and Applied Mathematics

journal homepage: www.elsevier.com/locate/cam

Asymmetric periodic orbits in the photogravitational Copenhagen problem

K. Papadakis [a,*], O. Ragos [b], C. Litzerinos [a]

[a] Department of Engineering Sciences, University of Patras, GR-26504 Patras, Greece

[b] Department of Mathematics, University of Patras, GR-26504 Patras, Greece

ARTICLE INFO

Article history:
Received 23 October 2007
Received in revised form 16 April 2008

Keywords:
Asymmetric orbit
Critical orbit
Levi-Civita regularization
Numerical integration
Periodic orbit
Radiation pressure
Three-body problem

ABSTRACT

In this paper we study the O*x*-asymmetric solutions of the planar photogravitational restricted three-body problem in the case of primaries with equal masses and equal values of the radiation pressure parameters. In particular, we are concerned with the families of asymmetric orbits which bifurcate from the well known families a, b, and c. Their evolution is examined via the numerical construction of series of the critical bifurcation points of a, b, and c with respect to the variation of the common radiation parameter q. We also present some illustrative cases of these families for several values of this parameter. In order to avoid the singularity due to binary collisions between the third body and one of the primaries, the equations of motion of the problem are regularized by using the Levi-Civita transformations.

1. Introduction

In this paper we deal with the "Copenhagen case" of the planar photogravitational restricted three-body problem. By extending the corresponding case of the classical gravitational problem, we admit that the mass and radiation pressure parameters of the primaries are equal, i.e. $1-\mu=\mu=0.5$ and $q_1=q_2=q$. The factors q_1, q_2 are related to the notation of Schuerman [11] by $q_1=1-b_1$, $q_2=1-b_2$ where b_1, b_2 are the ratios of the magnitudes of radiation to gravitational forces due to the two primary bodies m_1 and m_2. This problem can be used to model the motion of small particles under the influence of binary stars.

Poynting [8] has stated that particles, such as small meteors or cosmic dust, are comparably affected by gravitational and light radiation forces as they approach luminous celestial bodies. The importance of the radiation influence on celestial bodies has been recognized by many scientists, especially in connection with the formation of concentrations of interplanetary and interstellar dust or grains in planetary and binary star systems, as well as the perturbations on artificial satellites. The expression of the total radiation force on a particle P due to a radiation source S was given in [10], from the standpoint of the theory of relativity. Robertson stated that considering only terms of the first order in $\mathbf{v}/c$ constituted a justifiable approximation, readily interpretable in classical mechanics and electrodynamics, to yield:

$$\mathbf{F}=\mathbf{F_1}+\mathbf{F}_2+\mathbf{F_3}, \tag{1}$$

where

$$\mathbf{F_1}=F_p\frac{\mathbf{R}}{R}, \qquad \mathbf{F_2}=-F_p\frac{\mathbf{v}\cdot\mathbf{R}}{cR}\frac{\mathbf{R}}{R}, \qquad \mathbf{F_3}=-F_p\frac{\mathbf{v}}{c}. \tag{2}$$

* Corresponding author.
E-mail addresses: k.papadakis@des.upatras.gr (K. Papadakis), ragos@math.upatras.gr (O. Ragos).

0377-0427/$ – see front matter © 2008 Elsevier B.V. All rights reserved.
doi:10.1016/j.cam.2008.07.006

F_p denotes the measure of the radiation pressure force, **R** is the position vector of P with respect to S, **v** the corresponding velocity vector and c the velocity of light. The quantity F_p is given by

$$F_p = \frac{3Lm}{16\pi R^2 psc}, \tag{3}$$

where L is the luminosity of the radiating body, while m, p and s are the mass, density and cross section of the particle, respectively. The first component $\mathbf{F_1}$ in Eq. (1) expresses the radiation pressure. The second one, $\mathbf{F_2}$, represents the Doppler shift owing to the motion of the particle. The third component $\mathbf{F_3}$ is due to the absorption and subsequent re-emission of part of the incident radiation. The last two forces constitute the so-called Poynting–Robertson effect [9]. In the present paper we consider only the influence of the radiation pressure [1].

In spite of the apparent symmetry, it is known that in the gravitational problem there are asymmetric solutions with respect to either one or both of the two axes Ox and Oy (see, for example, [13]). In this contribution we are particularly interested in the families of asymmetric periodic orbits which bifurcate from the families of a, b, and c (we use the same notation as in Hénon's paper [2]). In the gravitational case $q = 1$, these latter classes consist of periodic solutions which are symmetric with respect to the Ox axis. Their starting-points are the collinear equilibrium points L_2, L_3 and L_1, respectively, and each of these families contains exactly one critical orbit for which $a_h = 1$ and $b_h = 0$ (see Section 3). Any of these orbits is a bifurcation point of a family of periodic solutions which are not symmetric with respect to either Ox or both Ox and Oy.

The evolution of the afore-mentioned critical orbits is studied by means of the numerical construction of series with respect to the variation of the common radiation parameter q. The computation of these series is accomplished by using the method that has been introduced in [2,3]. One may suspect that, a priori, there is a physical limiting case for the existence of the bifurcation point of c. This is the value of the radiation pressure parameter $q^* = 1/8$, when its starting-point, L_1, coincides with the triangular equilibrium points L_4 and L_5 (for details, see [6]). We have studied the whole range between the gravitational case and this critical value. We have found that for some subregions of this range there are more than one critical members of c. We have seen that q^* is indeed a critical value for all these bifurcation points. Regarding the families a and b, we have found that their critical orbits, originally existing in the gravitational case, cease to exist at a value of q greater than q^*. For a small range of q just before this value, another bifurcation point appears in a and b. The data describing the evolution of the afore-named series are presented in tabular and graphical form.

To complete our study, we have used the members of these series as starting-points to compute the families of asymmetric periodic orbits that bifurcate with a, b and c, for several values of q. We give the data of some representative cases of these families, too.

1.1. Equations of motion

Consider the motion of an infinitesimal mass that is influenced by the gravitational and radiation pressure forces of two illuminating primary bodies of mass m_1 and m_2 and radiation pressure factors q_1 and q_2. The two heaviest bodies (the primaries) revolve under their mutual gravitational attraction around their center of mass in circular orbits. The units of measure of mass, length and time are taken so that the sum of the masses and the distance between the primaries is unity, and, also, the Gaussian constant of gravitation G is 1. A rotating rectangular coordinate system whose origin is the center of mass of the primaries and whose Ox-axis contains the primaries is used. The angular velocity of the system is also unity (for details see [14]). Then, in this coordinate system the corresponding dimensionless equations of motion are written as follows [12]:

$$\ddot{x} - 2\dot{y} = \frac{\partial \Omega}{\partial x}, \qquad \ddot{y} + 2\dot{x} = \frac{\partial \Omega}{\partial y}, \tag{4}$$

where dots denote time derivatives. Ω stands for the photogravitational potential in synodic coordinates and it is given by

$$\Omega = \frac{1}{2}(x^2 + y^2) + \frac{q_1(1-\mu)}{r_1} + \frac{q_2\mu}{r_2}, \tag{5}$$

where $1 - \mu$ and μ are the mass ratios of m_1 and m_2 to $m_1 + m_2$, respectively, and r_i are the distances

$$r_1 = \sqrt{(x+\mu)^2 + y^2}, \qquad r_2 = \sqrt{(x+\mu-1)^2 + y^2}. \tag{6}$$

In our case, $1 - \mu = \mu = 0.5$ and $q_1 = q_2 = q$.

The energy integral of this problem is given by the expression

$$C = 2\Omega - (\dot{x}^2 + \dot{y}^2), \tag{7}$$

where C is the Jacobian constant.

1.2. Regularized equations of motion

During the computation of the series and the families, we had, in many cases, to compute orbits which were close to the vicinity of singularities of the problem. In these cases, we regularized the equations of motion by applying the transformations of Levi-Civita [4,14]. These transformations can be introduced as follows. Consider the relations

$$z = f(w), \qquad \frac{\mathrm{d}t}{\mathrm{d}\tau} = g(w) = |f'(w)|^2 \tag{8}$$

which connect the original coordinate system and the time variable

$$z = x + \mathrm{i}y \quad \text{and} \quad t, \tag{9}$$

(i is the imaginary unit) to the new variables

$$w = u + \mathrm{i}v \quad \text{and} \quad \tau, \tag{10}$$

where

$$f(w) = \mu + w^2 \quad \text{or} \quad f(w) = \mu - 1 + w^2. \tag{11}$$

If the first formula is applied for f, the singularity at the primary body of mass m_1 is regularized, while, if the second one is used, the singularity at m_2 is eliminated. Then, in the first case, the regularized equations of motion are

$$u'' - 8(u^2 + v^2)v' = \frac{\partial \Omega^*}{\partial u}, \qquad v'' + 8(u^2 + v^2)v' = \frac{\partial \Omega^*}{\partial v}, \tag{12}$$

where primes denote time derivatives with respect to the new time τ. The function of the photogravitational potential in regularized coordinates is given by

$$\Omega^* = 2(u^2 + v^2)\left\{-C + (2uv)^2 + (u^2 - v^2 + \mu)^2 + \frac{2q_1(1-\mu)}{\left[(2uv)^2 + (u^2 - v^2 + 2\mu)^2\right]^{1/2}} + \frac{2q_2\mu}{\left[(2uv)^2 + (u^2 - v^2 + 2\mu - 1)^2\right]^{1/2}}\right\}. \tag{13}$$

The Jacobian constant value is common in the two systems. In the new system, it can be obtained by

$$C = (u'^2 + v'^2) = 2\Omega^*. \tag{14}$$

The afore-mentioned transformation can easily been reversed. The original time t is obtained by a single integration of the time transformation:

$$t = \int^{\tau} g(w)\mathrm{d}\tau, \tag{15}$$

while the coordinates x and y are given by

$$x = u^2 - v^2 + \mu \quad \text{and} \quad y = 2uv. \tag{16}$$

The relations corresponding to the transformation which eliminates the singularity at the primary body of mass m_2 are similar.

2. The family network

In this section we present the network of the planar symmetric simple-periodic orbits of the classical restricted three-body problem as they have been illustrated in [7]. By the term "symmetric simple-periodic orbits" we mean the period-1 solutions which have two perpendicular intersections with the horizontal Ox-axis. In the Copenhagen case, there are twenty two families which are classified in three groups. The first group consists of pairs of families whose members are symmetric to each other with respect to the origin. The second one contains families whose members are symmetric with respect to the Oy-axis. The families which belong to the third group have the following property: for each periodic orbit of any of these families with Jacobian constant C, there is a symmetric solution with respect to the Oy-axis which belongs to the same family and corresponds to the same value of the Jacobian constant. Fig. 1 presents the network that is formed by these families for $q = 1$. The fundamental families a, b and c are included in this network. The families a and b consist of retrograde solutions around L_2 end L_3, respectively, and they belong to the first group, i.e. for a given periodic orbit of the first family, one may obtain a symmetric orbit which belongs to the second one, by replacing x, y and μ by $-x$, $-y$ and $1 - \mu$, and vice-versa. Family c consists of retrograde solutions around L_1 and belongs to the second group.

We remark that, in Fig. 1, as well as in all the data representations which are given in this paper, only those parts of the families which represent simple-periodic orbits are given. The family characteristic curves may continue with parts corresponding to higher-multiplicity orbits which appear after collision solutions with one of the primaries, but these parts are not considered in this paper.

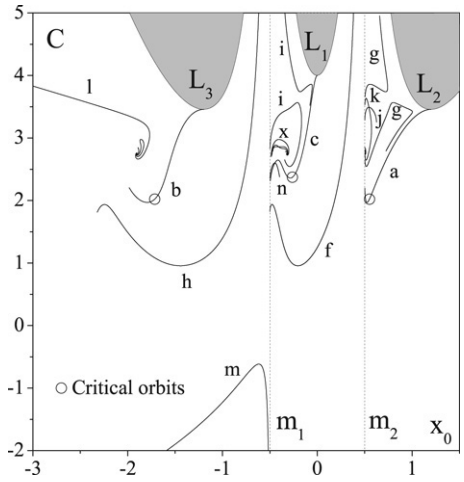

Fig. 1. The network of the families of the simple symmetric periodic solutions of the classical restricted three-body problem. Small circles indicate the critical periodic orbits ($a_h = 1$, $b_h = 0$) which are given by the first entries in Tables 1 and 2.

Table 1
The series, with respect to the radiation parameter q, of critical periodic orbits ($a_h = 1$, $b_h = 0$) of the family b

q	x_0	x_1	$T/2$	C
1.0	−1.71555788	−0.54973450	2.89508541	2.02078683
0.9	−1.65423664	−0.54116423	2.87621884	1.84732407
0.8	−1.58742265	−0.53220019	2.85434619	1.66660773
0.7	−1.51363274	−0.52289059	2.82862262	1.47708066
0.6	−1.43055580	−0.51344303	2.79786439	1.27633591
0.5	−1.33410663	−0.50462341	2.76045357	1.06002398
0.4	−1.21467874	−0.50008147	2.71481830	0.81699447
0.323493	−1.05121053	−0.54532783	2.68181192	0.53617102
0.397547	−0.85286119	−0.85286119	2.70576395	0.48489815

Table 2
A series, with respect to the radiation parameter q, of critical periodic orbits ($a_h = 1$, $b_h = 0$) of family c

q	$x_0\,(= -x_1)$	$T/2$	C
1.0	−0.26244069	2.63087648	2.37166911
0.9	−0.25540454	2.63030912	2.21393119
0.8	−0.24761727	2.63209761	2.04817200
0.7	−0.23882563	2.63729051	1.87301444
0.6	−0.22861934	2.64761066	1.68660412
0.5	−0.21627271	2.66609874	1.48633231
0.4	−0.20033150	2.69868437	1.26830458
0.3	−0.17725424	2.75881792	1.02618644
0.2	−0.13456609	2.88646856	0.74814705
1/8	0.0	3.14159265	0.5

This series starts from the critical point which is contained in this family when $q = 1$.

3. The evolution of the critical solutions

In this section we describe the evolution of the critical solutions (with $a_h = 1$, $b_h = 0$) that belong to a, b and c. We note here that, Hénon in 1965 [2] defines the isoenergetic stability index $S_h = (a_h + d_h)/2$, where a_h, d_h are the horizontal coefficients from the variational matrix,

$$\begin{pmatrix} \Delta x \\ \Delta \dot{x} \end{pmatrix} = \begin{pmatrix} a_h & b_h \\ c_h & d_h \end{pmatrix} \begin{pmatrix} \Delta x_0 \\ \Delta \dot{x}_0 \end{pmatrix}. \tag{17}$$

Δx, $\Delta \dot{x}$ are constrained to maintain the value of the Jacobian constant C and $a_h = \partial x/\partial x_0$, $b_h = \partial x/\partial \dot{x}_0$, $c_h = \partial \dot{x}/\partial x_0$, $d_h = \partial \dot{x}/\partial \dot{x}_0$. For high accuracy (i.e. the accuracy of the numerical integration), we integrated the equations of motion simultaneously with equations of variation and for the calculation of the stability coefficients we used the relevant relations in [5]. The stability condition of an orbit is $-1 < S_h < 1$ and if the orbit is symmetric then we had $a_h = d_h$ while if the orbit is asymmetric $a_h \neq d_h$ in general. In the same work [2] it was shown that if and only if a_h takes the value 1 and at the same time $b_h = 0$ ($c_h \neq 0$), then the family of symmetric periodic orbits intersects another family of asymmetric periodic

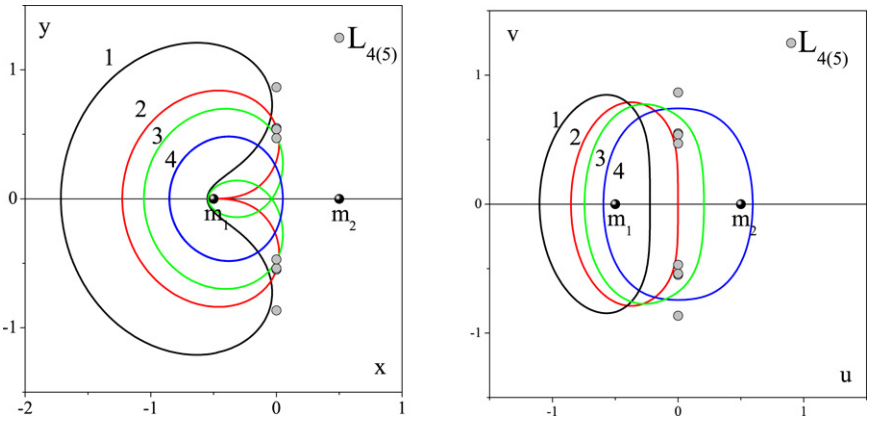

Fig. 2. Left: The evolution of the critical periodic orbit of the family b in the original (left) and in the regularized coordinate system (right) as the radiation factor varies: (1) $q = 1$, (2) $q = 0.409$, (3) $q = 0.32355$, and (4) $q = 0.397547$. Small circles indicate the positions of L_4 and L_5.

orbits. Using this critical periodic orbit, which belongs in both families, we can calculate the whole one-parameter family of asymmetric periodic orbits.

As has been already mentioned, the evolution of the critical solutions is studied via the numerical construction of series of these bifurcation points with respect to the variation of q. Namely, we consider that a plane orbit is periodic, symmetric (w.r.t. Ox-axis) and horizontally critical (here we are interested in $a_h = 1$) if the following conditions be simultaneously satisfied:

$$\begin{aligned} &y(x_0, \dot{y}_0, t; q) = 0 \\ &\dot{x}(x_0, \dot{y}_0, t; q) = 0 \\ &a_h(x_0, \dot{y}_0, t; q) = 1 \end{aligned} \tag{18}$$

at $t = T/2$. We expand Eq. (18) into Taylor series around $(x_0, \dot{y}_0, t)$ up to first order terms:

$$\begin{aligned} &\frac{\partial y}{\partial x_0}\delta x_0 + \frac{\partial y}{\partial \dot{y}_0}\delta \dot{y}_0 + \frac{\partial y}{\partial t}\delta t + \frac{\partial y}{\partial q}\delta q = -y, \\ &\frac{\partial \dot{x}}{\partial x_0}\delta x_0 + \frac{\partial \dot{x}}{\partial \dot{y}_0}\delta \dot{y}_0 + \frac{\partial \dot{x}}{\partial t}\delta t + \frac{\partial \dot{x}}{\partial q}\delta q = -\dot{x}, \\ &\frac{\partial a_h}{\partial x_0}\delta x_0 + \frac{\partial a_h}{\partial \dot{y}_0}\delta \dot{y}_0 + \frac{\partial a_h}{\partial t}\delta t + \frac{\partial a_h}{\partial q}\delta q = 1 - a_h. \end{aligned} \tag{19}$$

The partial derivatives $\partial y/\partial q$, $\partial \dot{x}/\partial q$ and $\partial a_h/\partial q$ are computed by using additional integrations while the rest of the coefficients of system (19) are obtained by the integration of the equations of variation. Then, we consider the value of q to be fixed, i.e. $\delta q = 0$, and thus we are able to compute the quantities δx_0, $\delta \dot{y}_0$ and δt by solving the system (19). We use then, the initial conditions vector $(x_0 + \delta x_0, 0, 0, \dot{y}_0 + \delta \dot{y}_0)$ and half period $t + \delta t$, and repeat the process until the conditions (18) are satisfied within the desired accuracy, say $\epsilon \leq 10^{-8}$. If a particular critical solution is known for a given value of q, a new one for $q + \delta q$ can be predicted by solving Eq. (19) again, after setting $y = \dot{x} = 1 - a_h = 0$. The independent conditions that must be satisfied are one less than the number of variables involved. This shows that the bifurcations actually form a one-parameter family which we shall call a "series" of periodic orbits.

In the gravitational case, each of the families a, b and c contains exactly one critical point. These orbits are denoted by small circles in Fig. 1.

Table 1 and Fig. 2 present the evolution of the bifurcation point of b. In Table 1, for each member of the series, we give the positions of the infinitesimal mass on the Ox-axis, x_0 and x_1, at $t = 0$ and $t = T/2$ as well as the values of the half-period and the Jacobian constant.

In the left part of Fig. 1, the orbit named by (1) represents the period-1 critical orbit of b when $q = 1$. The orbit marked by (2) is the bifurcation point of b for $q = 0.409$ and it is still a solution of period 1. The solution indicated by (3) is a period-2 critical solution when $q = 0.32355$. Then, for smaller values of q, the size of the inner loop of the members of the series increases until, finally, for $q = 0.397547$ we have the period-2 solution (4) whose loops coalesce. This is the termination point of the series and it coincides with a member of the family h. As can be seen in the right-hand frame of Fig. 2, in the regularized coordinate system, the multiplicity of all the critical orbits are 1. For any value of q in the range from 1 to 0.397547, family b continues to contain exactly one critical solution ($a_h = 1$ and $b_h = 0$). In the range from 0.397547 to 0.323493, another critical orbit appears in b (see the left frame of Fig. 4).

The evolution of the critical points of family a is analogous to that of b, since, as has been mentioned before, it consists of orbits which are symmetric, with respect to the origin O, with the members of the latter family. Thus, the termination point

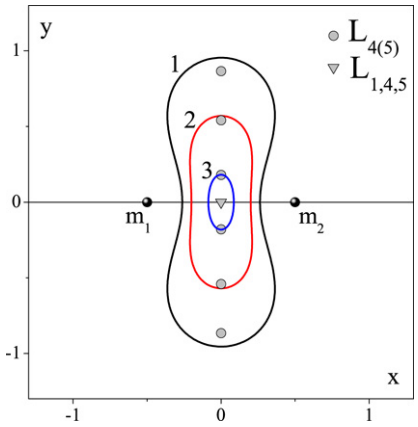

Fig. 3. The evolution of the critical periodic orbit, which originally exists in family c when $q = 1$, c as the radiation factor varies: (1) $q = 1$, (2) $q = 0.4$, and (3) $q = 0.15$. Small circles indicate the positions of L_4 and L_5. The small triangle indicates the common position of L_1, L_4 and L_5 when $q = q^*$.

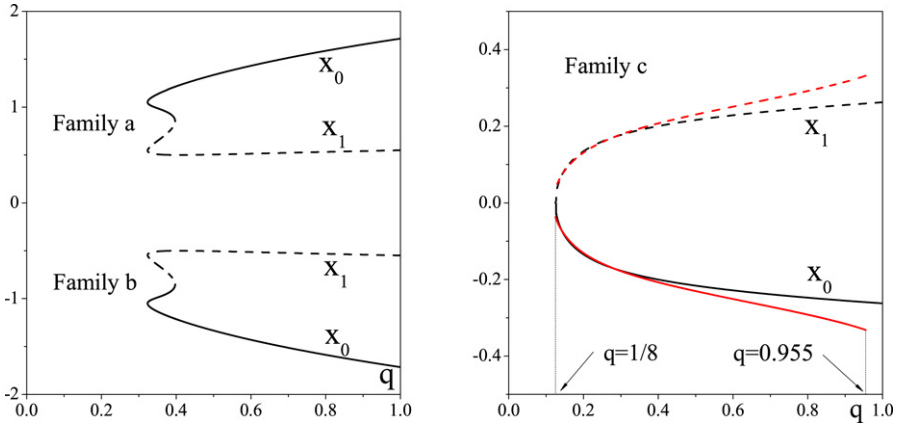

Fig. 4. The positions x_0 ($t = 0$, solid lines) and x_1 ($t = T/2$, dashed lines) of the critical periodic orbits ($a_h = 1$, $b_h = 0$) of families a, b (left) and c (right).

of the series corresponding to a is a critical orbit of h which is O-symmetric with the end-point of the series related to b (see Fig. 4).

The critical orbit which originally is contained in the family c for $q = 1$ continues to exist until $q = q^*$. Its evolution with respect to q is presented in Table 2 and Fig. 3. The corresponding series consists of period−1 symmetric orbits whose size gradually decreases until, finally, this series terminates on L_1.

The afore-mentioned series of critical solutions of the family c is not unique. As we will see in Section 4.2, for values of the parameter q less than 0.955, this family contains more critical orbits. For these values of q, family c starts from the collinear equilibrium point L_1 and it has as terminal points asymptotic solutions which intersect the Ox-axis perpendicularly and spiral to L_4 for $t \to +\infty$ and to L_5 for $t \to -\infty$ (for details, see [7]).

We note here that, in the circular restricted three-body problem for decreasing values of the radiation factors q_1, q_2, the triangular equilibrium points L_4, L_5 approach the inner collinear point L_1 and finally disappear by coalescing on the axis and transferring their stability to L_1 at the same time [12]. When $q_1 = q_2 = q$, this occurs at the critical value of the common radiation factor $q^* = 1/8$ [6].

The characteristic curve (x_0, C) of the family c also spirals asymptotically to a point with $C = C_{L_{4,5}}$. Along each loop of this spiral there is a critical solution of c. We calculated the series, with respect to the variation parameter q, of the critical periodic orbits and we found that the afore-mentioned characteristic curve retains this behavior for $0.955 \geq q \geq 0.14$. So, theoretically, for each of these values of q, the family c may contain an infinite number of bifurcation points with families of asymmetric periodic orbits. If q is smaller than 0.14 but greater than q^*, there are exactly two critical solutions in the family c. We have seen that one of these solutions results from the bifurcation point that exists in c when $q = 1$. The evolution of the second critical solution of c that persists throughout the whole range from 0.955 to q^* is represented in Table 3. The shapes of the members of the corresponding series are almost alike to those given in Fig. 2. For $q < q^*$, one critical orbit exists on the "Short"-family that starts from $L_{1,4,5}$.

Table 3
Another series, with respect to the radiation parameter q, of critical periodic orbits ($a_h = 1$, $b_h = 0$) of the family c

q	$x_0\ (= -x_1)$	$T/2$	C
0.955	−0.33179341	6.16472801	2.72677099
0.9	−0.31577097	6.12020973	2.60447449
0.8	−0.29198680	6.04754239	2.38018634
0.7	−0.27110771	5.98210494	2.14973073
0.6	−0.25108033	5.92423804	1.91023469
0.5	−0.23045895	5.87799828	1.65873290
0.4	−0.20741814	5.85443733	1.39127733
0.3	−0.17827074	5.88550058	1.10173368
0.2	−0.13115529	6.10260555	0.77889489
1/8	−0.03701696	7.03027714	0.50039431

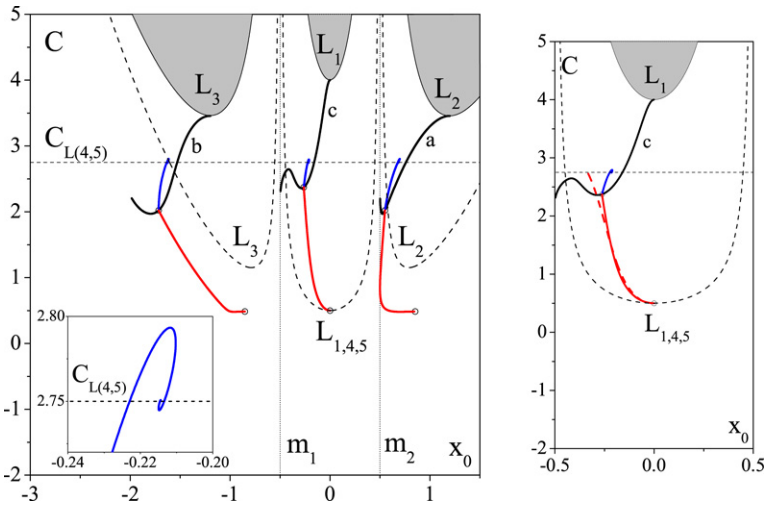

Fig. 5. Left: Characteristic curves, in the (x_0, C) plane, of the families a, b and c (black lines) and the families of asymmetric periodic orbits which bifurcate from them (blue lines) in the gravitational restricted three-body problem ($q = 1$). The evolution of the critical periodic orbits of a, b and c, with respect to the radiation factor q, is also given (red lines). In the inner window, a zoom of the end of one of the families of asymmetric orbits bifurcating from c is illustrated. The borders of shaded areas represent the zero-velocity curves when $q = 1$. The dotted lines are the zero velocity curves when the radiation factor is $q = 1/8$. Right: A magnification of the area around L_1 where now a second series of critical periodic orbits of family c appears (red dashed line). (For interpretation of the references to colour in this figure legend, the reader is referred to the web version of this article.)

In Fig. 4, the variation of the intersections of the orbits of the afore-mentioned series with the Ox-axis is shown. In the left part of this figure, the series relative to the families a and b are presented. In the right part, we give the corresponding data for two series of critical points of the family c as well as the limiting values of q for their existence.

4. Families of asymmetric orbits

In this section we deal with the families of asymmetric orbits which bifurcate from the critical points of a, b and c. First, we present, for comparison purpose, these families in the classical gravitational problem when $q = 1$. Then, we describe the behavior of these families in the photogravitational one by giving and discussing their data for some illustrative cases of the radiation pressure factor.

4.1. Gravitational case

The left part of Fig. 5 represents the (x_0, C)-characteristic curves of the families a, b and c (black lines) along with those of the families of asymmetric periodic orbits that bifurcate from them (blue lines) when $q = 1$. The starting points of a, b and c are found in the vicinity of the local minima of the zero-velocity curves which are the borders of the shaded areas. The series of the bifurcation points of a, b and c are also shown in this figure (red lines) together with the zero-velocity curves for $q = q^*$ (dotted lines).

As can be seen, the three families of asymmetric orbits end by spiraling to points whose Jacobian constant value equals that of the triangular equilibrium points. So, the termination points of these families are homoclinic asymptotic solutions of L_4 or L_5. A magnification of the vicinity of the termination point of the family of asymmetric orbits bifurcating from c is shown in the inner window.

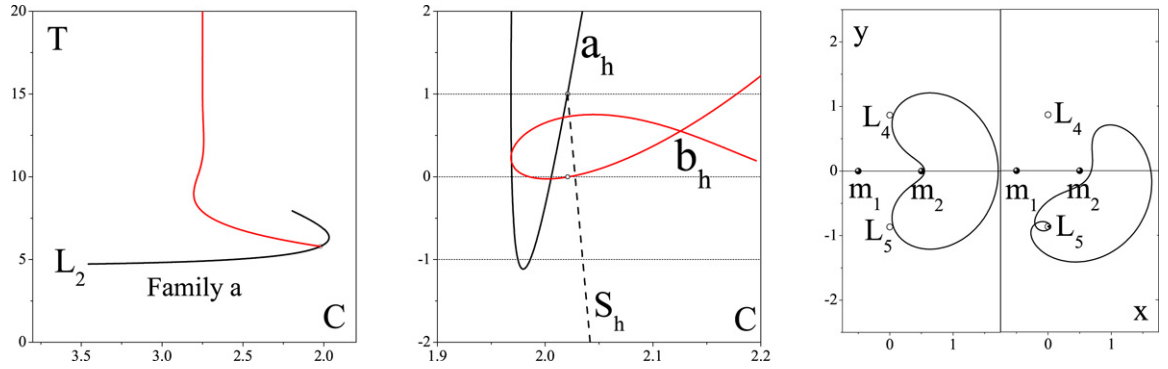

Fig. 6. Left: The (C, T) characteristic curves of family a (black line) and the family of asymmetric orbits which bifurcates from it (red line). Middle: The stability curves of a (solid line) and of its bifurcation (dotted line). Right (first frame): The critical orbit of family a. Right (second frame): A member of the family of asymmetric orbits near to one of its termination points. (For interpretation of the references to colour in this figure legend, the reader is referred to the web version of this article.)

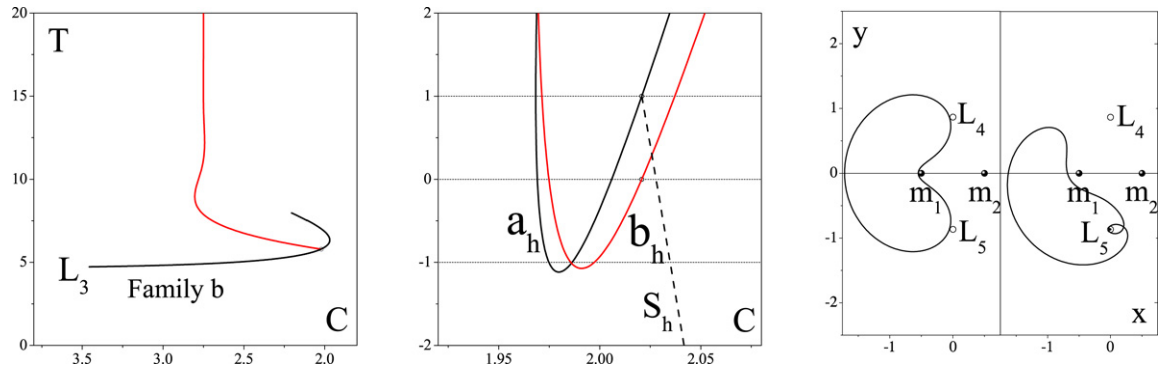

Fig. 7. Left: The (C, T) characteristic curves of family b (black line) and the family of asymmetric orbits which bifurcates from it (red line). Middle: The stability curves of b (solid line) and of its bifurcation (dotted line). Right (first frame): The critical orbit of family b. Right (second frame): A member of the family of asymmetric orbits near to one of its termination points. (For interpretation of the references to colour in this figure legend, the reader is referred to the web version of this article.)

In the left frame of Fig. 6, we present the (C, T) characteristic curve of family a (black line) and its bifurcating family of asymmetric periodic orbits (red line). In the middle frame, the horizontal stability diagram of these families is given. More precisely, the (C, a_h) and (C, b_h) characteristic curves of a are shown (continuous lines) together with the variation of the horizontal stability coefficient $S_h = (a_h + d_h)/2$ [3]. We note that the family of asymmetric solutions consists of unstable members except in a part near the bifurcation point. It is clear that the members of this family are asymmetric with respect to both axes and that its termination point is a homoclinic asymptotic orbit to L_5 (Fig. 6, right frame).

In Figs. 7 and 8 we present the corresponding data for the families b and c. Besides the expected symmetry of the results concerning the families a and b, one may notice that the family of asymmetric orbits bifurcating from c is also stable in its starting part and its termination points are homoclinic orbits to L_5. Its members are asymmetric with respect to the Ox-axis only.

4.2. Photogravitational case

Fig. 9 presents the (x, C)-characteristic curves of the families a, b and c (black lines) as well as those of the families of asymmetric periodic orbits that bifurcate from them (blue lines) when $q = 0.75$. Although the behavior of a and b is similar to that of the gravitational problem, this is not the case for family c. While, when $q = 1$, this family is heading for a collision with the primary m_1, for $q = 0.75$ the characteristic curve of c ends by spiraling to a point whose Jacobian constant value is equal to $C_{L_{4,5}}$. As has been mentioned in Section 3, for any loop of this spiral another critical orbit exists in this family. Here we present two families of asymmetric solutions which bifurcate from c: (a) the family which bifurcates from that critical orbit which emerges from the evolution of the bifurcation point contained in c when $q = 1$ and (b) the family that bifurcates from c from the critical point that exists in the first loop of the afore-mentioned spiral. In the inner frame of Fig. 9 it can be seen that both of these families (blue lines) terminate upon spiraling to points whose the Jacobian constant value is equal to $C_{L_{4,5}}$. The critical points are denoted by small circles.

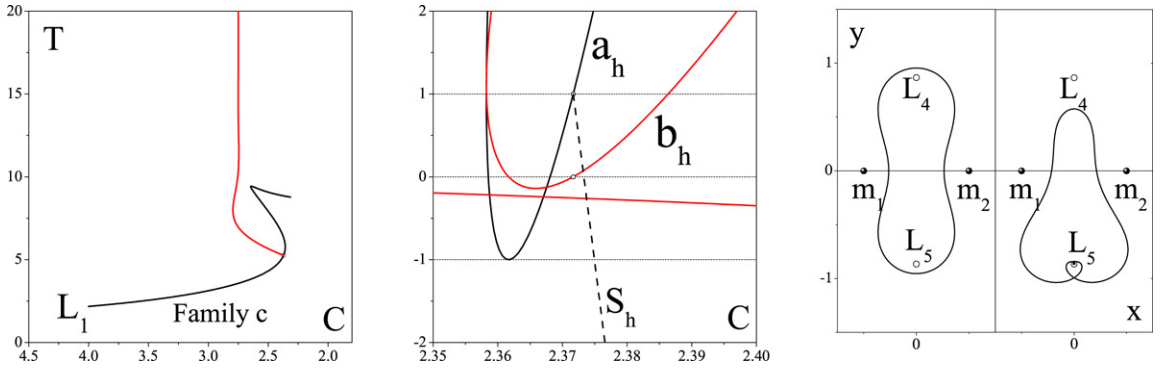

Fig. 8. Left: The (C, T) characteristic curves of family c (black line) and the family of asymmetric orbits which bifurcates from it (red line). Middle: The stability curves of c (solid line) and of its bifurcation (dotted line). Right (first frame): The critical orbit of family c. Right (second frame): A member of the family of asymmetric orbits near to one of its termination points. (For interpretation of the references to colour in this figure legend, the reader is referred to the web version of this article.)

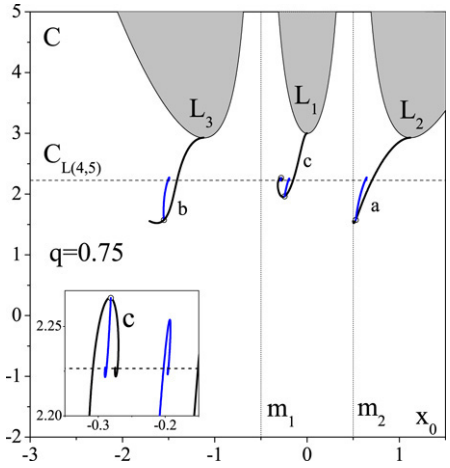

Fig. 9. Families a, b and c (black lines) and the families of asymmetric periodic bifurcating from them (blue lines) for $q = 0.75$. In the inner window, the end of c and its bifurcations is shown. (For interpretation of the references to colour in this figure legend, the reader is referred to the web version of this article.)

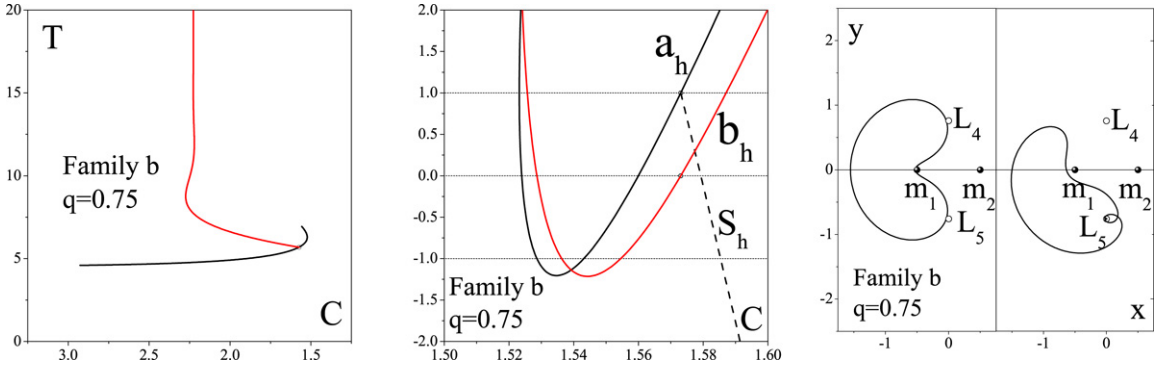

Fig. 10. Left: The (C, T) characteristic curves of family b (black line) and the family of asymmetric orbits which bifurcates from it (red line) for $q = 0.75$. Middle: The stability curves of b (solid line) and of its bifurcation (dotted line). Right (first frame): The critical orbit of family b. Right (second frame): A member of the family of asymmetric orbits near to its termination point. (For interpretation of the references to colour in this figure legend, the reader is referred to the web version of this article.)

In Fig. 10, the (C, T) characteristic curves, the stability diagrams and some indicative orbits of family b and its bifurcating family of asymmetric solutions are given. Because of symmetry, the behavior of family a is analogous to that of b and will not be discussed.

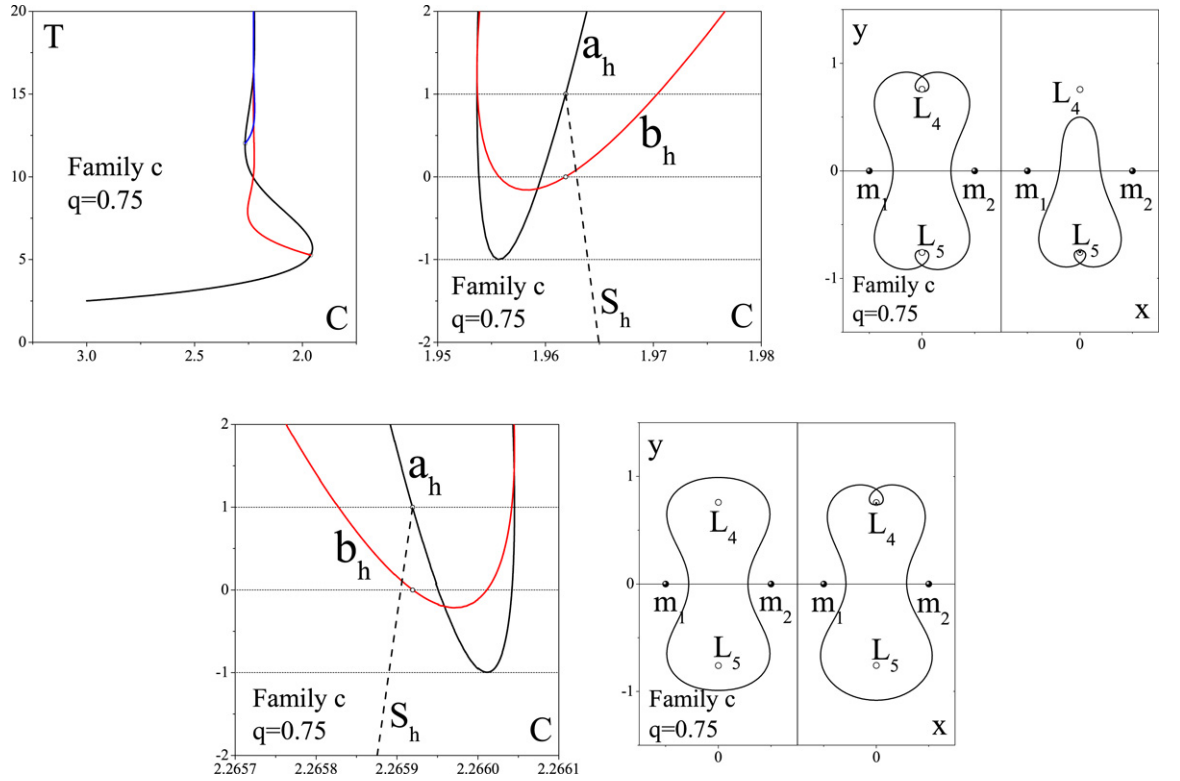

Fig. 11. Upper left: The (C, T) characteristic curves of family c (black line) and two of the families of asymmetric orbits which bifurcate from it (blue and red lines) for $q = 0.75$. Upper middle: The stability curves of c (solid line) and of its first bifurcation (dotted line). Upper right: The critical orbit of family c and a member of the family of asymmetric orbits near to its termination point. Lower left: The stability curves of c (solid line) and of its second bifurcation (dotted line). Lower right: The critical orbit of family c and a member of the family of asymmetric orbits near to its termination point. (For interpretation of the references to colour in this figure legend, the reader is referred to the web version of this article.)

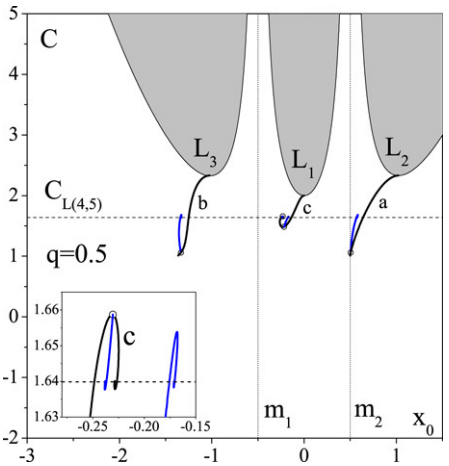

Fig. 12. Families a, b and c (black lines) and the families of asymmetric periodic bifurcating from them (blue lines) for $q = 0.5$. In the inner window, the end of c and its bifurcations is shown. (For interpretation of the references to colour in this figure legend, the reader is referred to the web version of this article.)

Fig. 11 represents the corresponding data for family c. In the upper left frame, family c (black line) and the bifurcating families (blue and red lines) are shown together. In the other two upper frames, c is presented along with the first family of asymmetric orbits while the lower frames are devoted to the family c and its second bifurcation. The termination points of the first and the second bifurcations of c are homoclinic asymptotic orbits to L_5 and L_4, respectively. The evolution of the rest of the families of asymmetric solutions bifurcating from c is qualitatively similar to that of either the first or the second one.

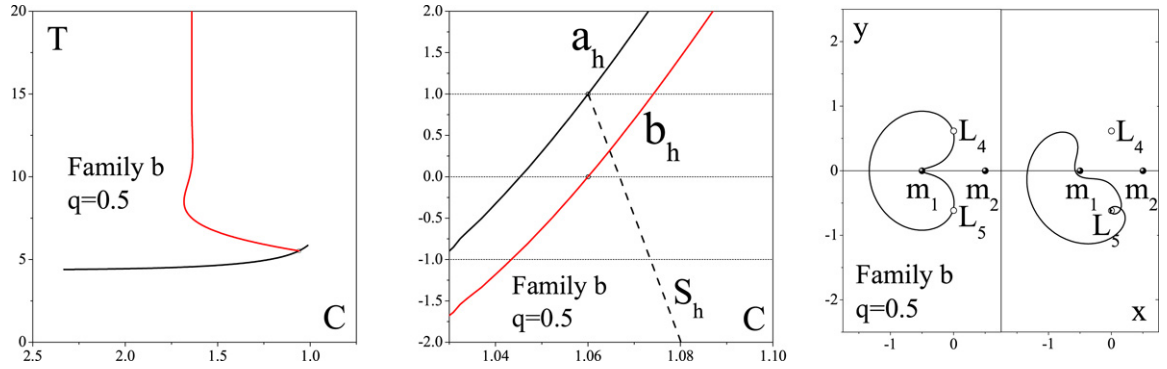

Fig. 13. Left: The (C, T) characteristic curves of family b (black line) and the family of asymmetric orbits which bifurcates from it (red line) for $q = 0.5$. Middle: The stability curves of b (solid line) and of its bifurcation (dotted line). Right (first frame): The critical orbit of family b. Right (second frame): A member of the family of asymmetric orbits near to its termination point. (For interpretation of the references to colour in this figure legend, the reader is referred to the web version of this article.)

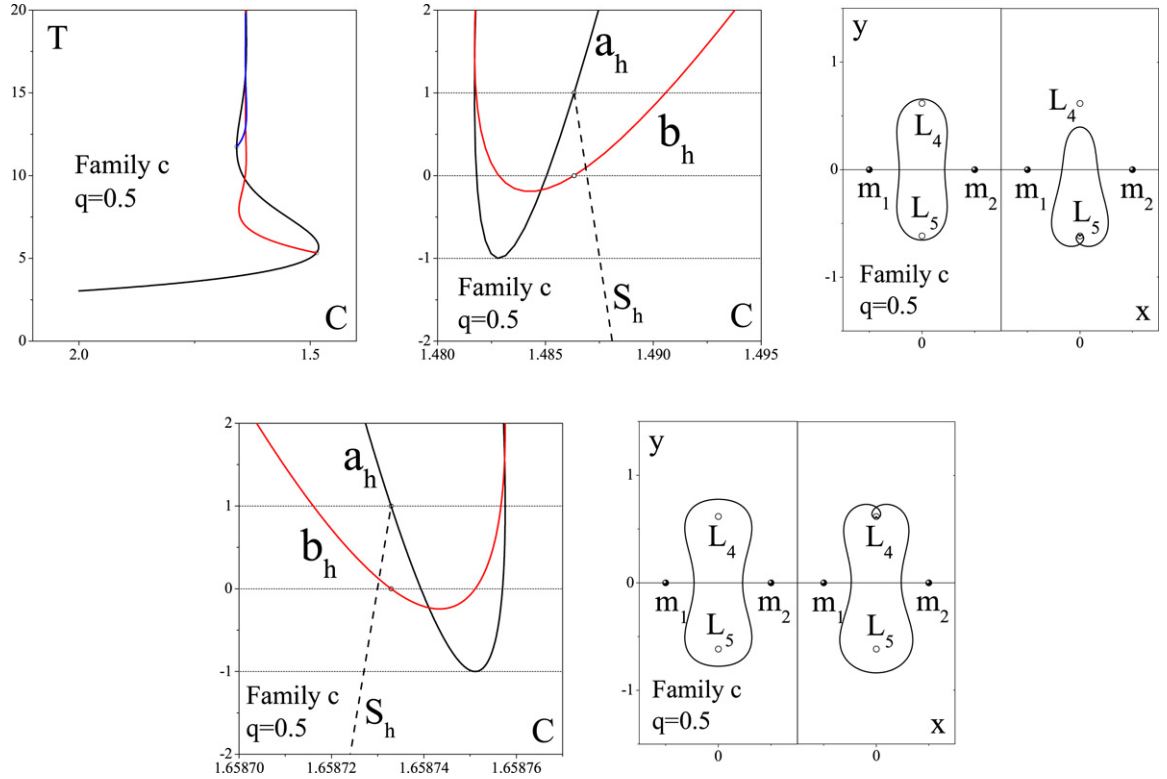

Fig. 14. Upper left: The (C, T) characteristic curves of family c (black line) and two of the families of asymmetric orbits which bifurcate from it (blue and red lines) for $q = 0.25$. Upper middle: The stability curves of c (solid line) and of its first bifurcation (dotted line). Upper right: The critical orbit of family c and a member of the family of asymmetric orbits near to its termination point. Lower left: The stability curves of c (solid line) and of its second bifurcation (dotted line). Lower right: The critical orbit of family c and a member of the family of asymmetric orbits near to its termination point. (For interpretation of the references to colour in this figure legend, the reader is referred to the web version of this article.)

In Figs. 12–14 we present the behavior of a, b, and c and their bifurcating families of asymmetric solutions for $q = 0.5$. The picture is qualitatively the same as in the previous case. The size of the members of c and its bifurcations are smaller now, since they surround L_1 while L_4, L_5 are closer to this equilibrium point. Fig. 15 represents the status of a, b, and c and their bifurcating families of asymmetric solutions for $q = 0.25$. The situation is quite different in this case for the families a and b since they contain no critical orbits any more. On the contrary, c contains many such solutions. The behavior of the first two is shown in Fig. 16. The members of family c look like those of the previous case.

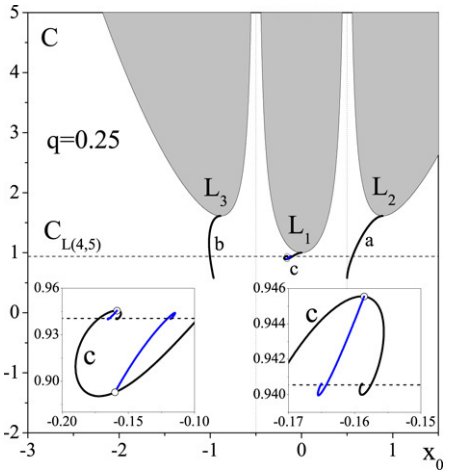

Fig. 15. Families a, b and c (black lines) and the families of asymmetric periodic bifurcating from them (blue lines) for $q = 0.25$. In the inner windows, the end of c and its bifurcations is shown. (For interpretation of the references to colour in this figure legend, the reader is referred to the web version of this article.)

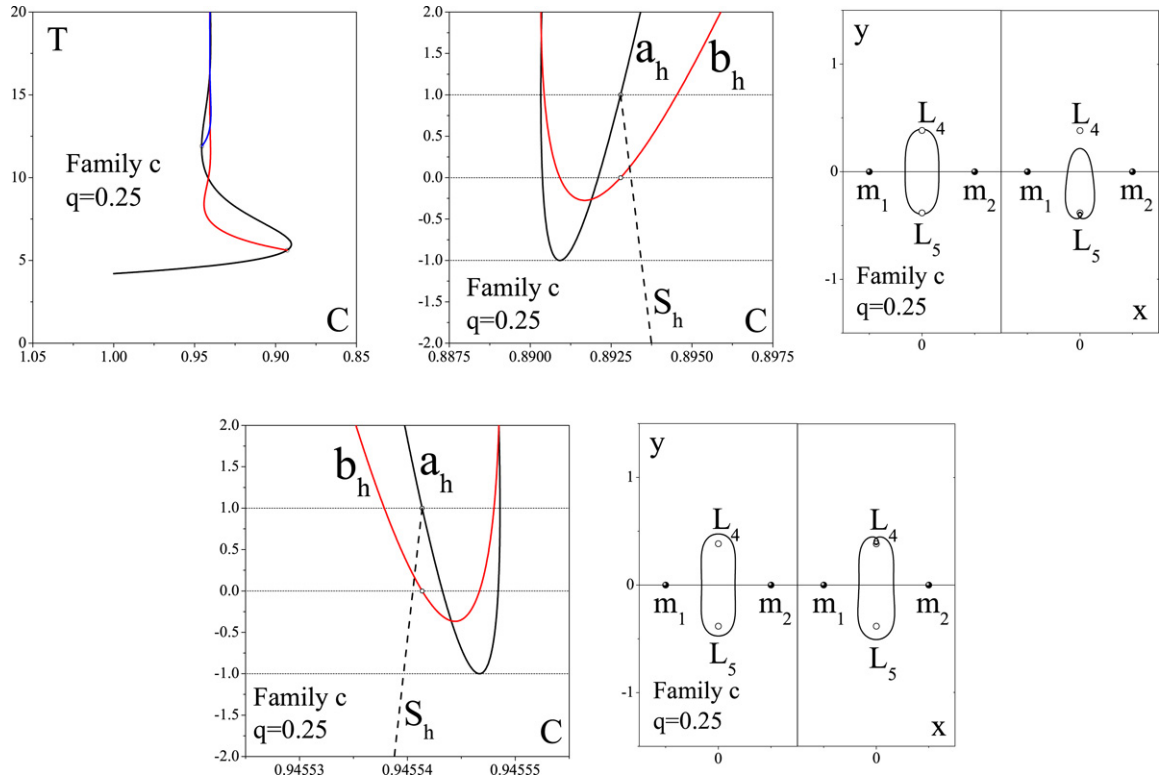

Fig. 16. Upper left: The (C, T) characteristic curves of family c (black line) and two of the families of asymmetric orbits which bifurcate from it (blue and red lines) for $q = 0.25$. Upper middle: The stability curves of c (solid line) and of its first bifurcation (dotted line). Upper right: The critical orbit of family c and a member of the family of asymmetric orbits near to its termination point. Lower left: The stability curves of c (solid line) and of its second bifurcation (dotted line). Lower right: The critical orbit of family c and a member of the family of asymmetric orbits near to its termination point. (For interpretation of the references to colour in this figure legend, the reader is referred to the web version of this article.)

5. Conclusions

In this contribution, we study the evolution of the families of symmetric solutions a, b and c, their critical points ($a_h = 1$, $b_h = 0$) as well as the families of asymmetric orbits which bifurcate from them, when the gravitation and radiation pressure forces of the two primaries are equal. This evolution was examined for values of the radiation factor in the whole range of q. The main results of this study are the following:

• The number of the critical orbits of the families a, b and c depends on the value of q.

• Families a and b contain exactly one such solution each for all values of q in the range $q = 1$ to $q = 0.397547$. When q varies between 0.397547 and 0.323493, another critical orbit appears in these families. The series of critical orbits of a and b terminate on a member of family h. For values of q less than 0.323493, a and b possess no critical orbits.

• Family c contains exactly one critical orbit for values of the radiation pressure parameter in the range $q = 1$ to 0.955. For $0.995 \leq q \leq 0.14$ c contains more such solutions whose number tends to ∞. For $q < 0.14$ and $q > 1/8$, c contains two critical points. If $q \leq 1/8$, one of these points persists on family "Short".

• The (x, C) characteristic curves of all the families of asymmetric solutions that bifurcate from a, b or c spiral to points whose the Jacobian constant value is equal to $C_{L_{4,5}}$.

• The termination points of all the families of asymmetric solutions that bifurcate from a, b or c are homoclinic asymptotic solutions to L_4 or L_5. More precisely, when $\dot{x}_0 > 0$, these termination orbits are asymptotic to one of the triangular equilibrium points while, when $\dot{x}_0 < 0$, they are asymptotic to the other point.

• The families of asymmetric orbits which bifurcate from a or b consist of member which are not symmetric to both the axes Ox and Oy.

• The families of asymmetric orbits which bifurcate from c are composed of members which are not symmetric to the Ox axis only.

• All the members of the families of asymmetric orbits that bifurcate from a, b or c are unstable except for those which are in the vicinity of their bifurcation points.

References

[1] Y.A. Chernikov, The photogravitational restricted three-body problem, Soviet Astron. - A.J. 14 (1970) 176–181.
[2] M. Hénon, Exploration numérique du problème restreint. II Masses égales, stabilité des orbites périodiques, Ann. Astrophys. 28 (1965) 992–1007.
[3] M. Hénon, Families of asymmetric periodic orbits in Hill's problem of three bodies, Celest. Mech. Dyn. Astr. 93 (2005) 87–100.
[4] T. Levi-Civita, Sur la résolution qualitative du probléme des trois corps, Acta Math. 30 (1906) 305–327.
[5] V.V. Markellos, On the stability parameters of periodic solutions, Astrophys. Spac. Sci. 43 (1976) 449–458.
[6] V.V. Markellos, E.A. Perdios, K.E. Papadakis, The stability of inner collinear equilibrium points in the photogravitational elliptic restricted problem, Astrophys. Spac. Sci. 199 (1993) 139–146.
[7] K.E. Papadakis, Families of periodic orbits in the photogravitational three-body problem, Astrophys. Spac. Sci. 245 (1996) 1–13.
[8] J.H. Poynting, Radiation in the solar system: its effect on temperature and its pressure on small bodies, Philos. Trans. Roy. Soc. London 202 (1903) 525–552.
[9] O. Ragos, F.A. Zafiropoulos, A numerical study of the influence of the Poynting–Robertson effect on the equilibrium points of the photogravitational restricted three-body problem, Astron. Astrophys. 300, 568–578.
[10] H.P. Robertson, Dynamical effects of radiation in the solar system, Monthly Not. Roy. Astr. Soc. 97 (1937) 423–438.
[11] D.W. Schuerman, The restricted three-body problem including radiation pressure, Astrophys. J. 238 (1980) 337–342.
[12] J.F.L. Simmons, A.J.C. McDonald, J.C. Brown, The restricted 3-body problem with radiation pressure, Celest. Mech. 35 (1985) 145–187.
[13] E. Strömgren, Forms of periodic motion in the restricted problem and in the general problem of three bodies, according to researches executed at the Observatory of Copenhagen, Copenhagen Obs. Publ. No. 39 (1922).
[14] V. Szebehely, Theory of Orbits, Academic Press, New York, 1967.